EXPERIMENTAL INVESTIGATION ON THE PUNCHING SHEAR BEHAVIOUR OF RC SLAB-COLUMN CONNECTIONS CONTAINING SHEAR STUDS UNDER SEISMIC LOADING

Amr Abdelkhalik Elsayed[1]
[1]*Assistant Professor, Civil Engineering Department, Badr University in Cairo, Cairo, EGYPT*
Email: amr.abdelkhalek@buc.edu.eg
Tel: +201008444069

ABSTRACT

Reinforced concrete flat slab-column structures are widely used because of their practicality. However, this type of structures can be subjected to punching-shear failure within the slab-column connections. Without shear reinforcement, the slab-column connection can undergo brittle punching failure, especially when the structure is subjected to lateral loading in seismic zones. The shear studs are an efficient good type of transverse reinforcement against punching failure. This research focuses on improving the punching shear capacity and ductility of the interior slab-column connections under constant vertical load in addition to cyclic loading using shear studs. The first specimen FP-GR-CTRL was tested subjected to vertical load only without cyclic loading while the other specimens FP-VR-0.4, FP-VR-0.6, FP-VR-0.8, FP-SS-0.4, FP-SS-0.6 and FP-SS-0.8 were tested under constant vertical load in addition to a reversed cyclic loading increased up to punching shear failure. The main objective is to discuss the effect of the shear studs on the punching shear behaviour. Finally, the experimental results are analyzed and compared to international codes such as American Code ACI318-14 and Euro Code EC2-2004. In light of these results, some preliminary conclusions are presented.

Keywords: Punching shear, shear studs, seismic loading, interior slab-column connections, gravity shear ratio, displacement control.

I. INTRODUCTION

Among many types of reinforced concrete buildings, reinforced concrete flat slab structure is very popular; it consists of flat plate and columns, with no beams between the columns to support the slab. The research addresses the behaviour and design of this type of structures. Emphasis is on the punching shear behaviour of slab-column connections by using shear studs in seismic zones.

Flat slab-column structural systems are popular due to reduction of building story height, easy setting up of formwork, convenience for utilities layout, and good slabs appearance. However, this type of structure can easily be subject to brittle punching shear failure. When the flat slab-column connections are subjected to heavy vertical loading, cracks will occur inside the slab in the vicinity of the column. These cracks then propagate through the slab thickness at an angle of 20 to 45 degree to the bottom of the slab [1-9]. This can lead to punching shear failure of the slab along the cracks. When subjected to seismic lateral load, shear stresses in the slab increase due to an unbalanced moment (from horizontal cyclic loading), and the slab-column Connection is more likely to fail by punching shear [10-15].

II. EXPERIMENTAL PROGRAM

A total of seven full scale specimens were tested. The specimen can be regarded as part a prototype structure of which the flat concrete slab spans 4.5 m between columns. The slab thickness is 200 mm. Figure 1 shows the concrete dimensions of all tested specimens while Figure 2 shows layout of shear studs for specimens with shear studs. The specimens represent interior slab-column connections, which are isolated specimens with dimensions corresponding to the lines of contra flexure under gravity loads. The control reference specimen FP-GR-CTRL, was subjected to a monotonic vertical load up to punching shear failure. Specimens without shear studs FP-VR-0.4, FP-VR-0.6 and FP-VR-0.8 were subjected to a constant vertical load V=230, 295 and 393 KN respectively, in addition to a reversed displacement controlled cyclic loading which was increased up to punching shear failure. Finally, all tested specimens with shear studs FP-SS-0.4, FP-SS-0.6 and FP-SS-0.8 were subjected to a constant vertical load V=195, 295 and 393 KN respectively, in addition to a reversed displacement controlled cyclic loading up to failure. The specimens FP-VR-0.4, FP-VR-0.6, FP-VR-0.8, FP-SS-0.4, FP-SS-0.6 and FP-SS-0.8 were subjected to constant gravity shear ratio V/V_0 equal 0.4, 0.6, 0.8, 0.4, 0.6 and 0.8 respectively, where V is the applied vertical load and V_0 is the vertical load causing punching shear failure according to ACI318-14 [16].

In the tension side of the concrete slab, the flexural reinforcement ratio is 1.62% within a width of 824 mm from the center of the slab as shown in Figure 3. The reinforcing ratio in the compression side of the slab is 0.6%. The reinforcement is designed by using first principles to ensure punching shear failure of these connections and not failure due to flexure. The reinforcing ratio of the columns is 4.86% and closed ties are used in order to make the column strong enough to transfer the axial load and unbalanced moment to the slab. Figure 3 shows the reinforcement details of all tested specimens. For control purposes, standard concrete cubes and cylinders were cast alongside the specimens and were tested at the same day as the specimen. The compressive cylinder concrete strengths for specimens FP-GR-CTRL, FP-VR-0.4, FP-VR-0.6, FP-VR-0.8, FP-SS-0.4, FP-SS-0.6, and FP-SS-0.8 equal 27, 35, 25, 25, 25, 25 and 25 N/mm^2 respectively. The main reinforcement and shear studs were made of deformed steel bars (Grade 40/60) of actual yield stress (F_Y) of 400 MPa, ultimate tensile strength f_u of 600 MPa and modulus of elasticity E_s of 200 GPA.

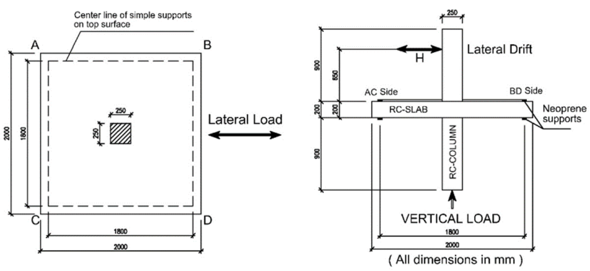

Figure 1: Concrete dimensions of all tested specimens

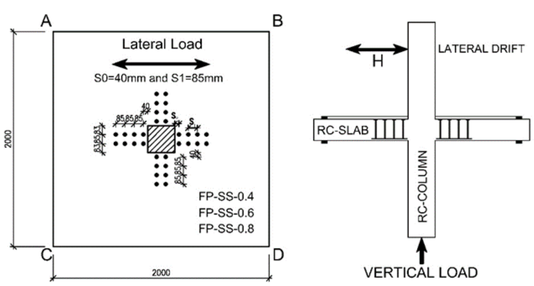

Figure 2: Layout of shear studs for specimens FP-SS-0.4, FP-SS-0.6 and FP-SS-0.8

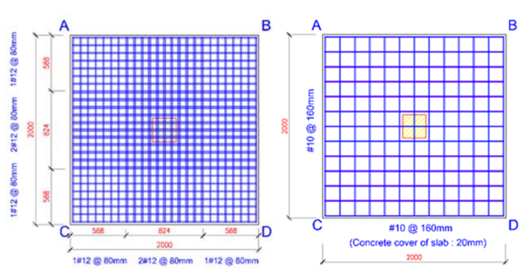

(a) Tensile reinforcement mesh (upper) (b) Compression reinforcement mesh (lower)

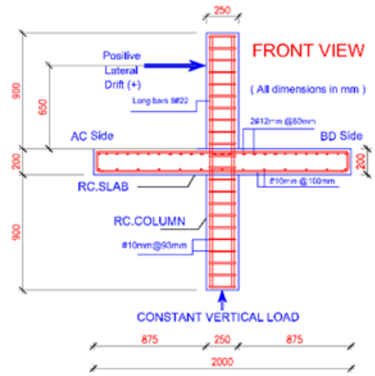

(c) Specimen reinforcement details

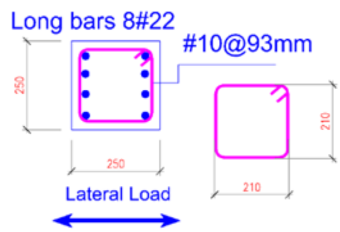

(d) Column reinforcement

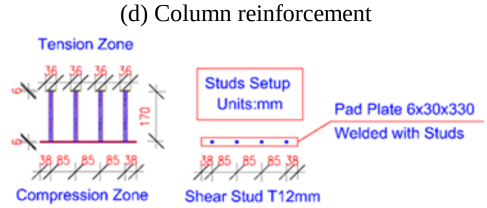

(e) Shear studs properties

Figure 3: Reinforcement details of all tested specimens

III. Test Setup, Boundary Conditions and Loading Scheme

Specimen FP-GR-CTRL was tested under vertical load only while all other specimens were tested under a constant vertical load, in addition to reversed cyclic load up to punching shear failure. Figure 4 shows a schematic of test set up of all specimens and the protocol cyclic loading path of tested specimens. Figure 5 shows the horizontal and vertical actuators as well as the digital recording computer system used to record the drift ratio versus the applied lateral load.

Figure 4: Schematic of test setup of tested specimens and cyclic loading path

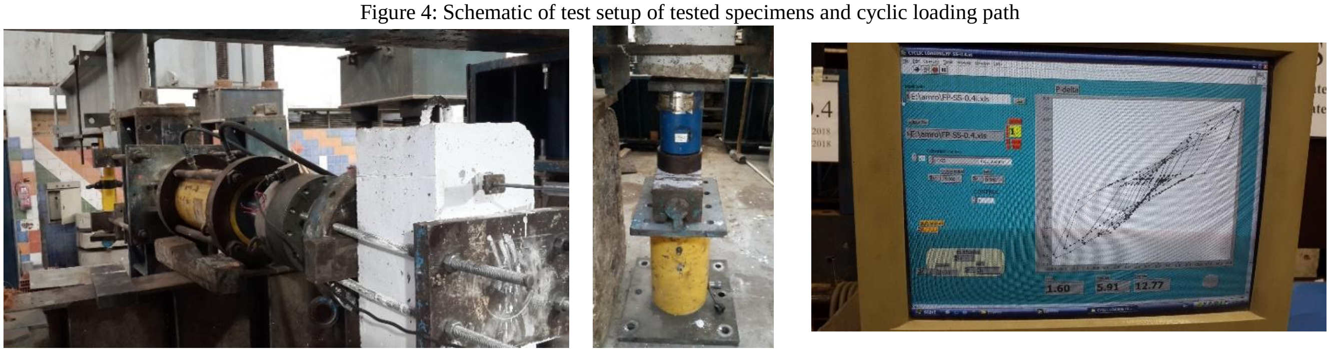

Figure 5: The horizontal-vertical actuator and digital recording computer system

IV. INSTRUMENTATION

Measurements were made thoroughly for displacements and steel strains at key locations of the tested specimens as shown as in Figures 6. All LVDTs and strain gauges were connected to a computer /controlled data acquisition system. The crack pattern was monitored and marked on the specimen with the associated load level indicated next to it.

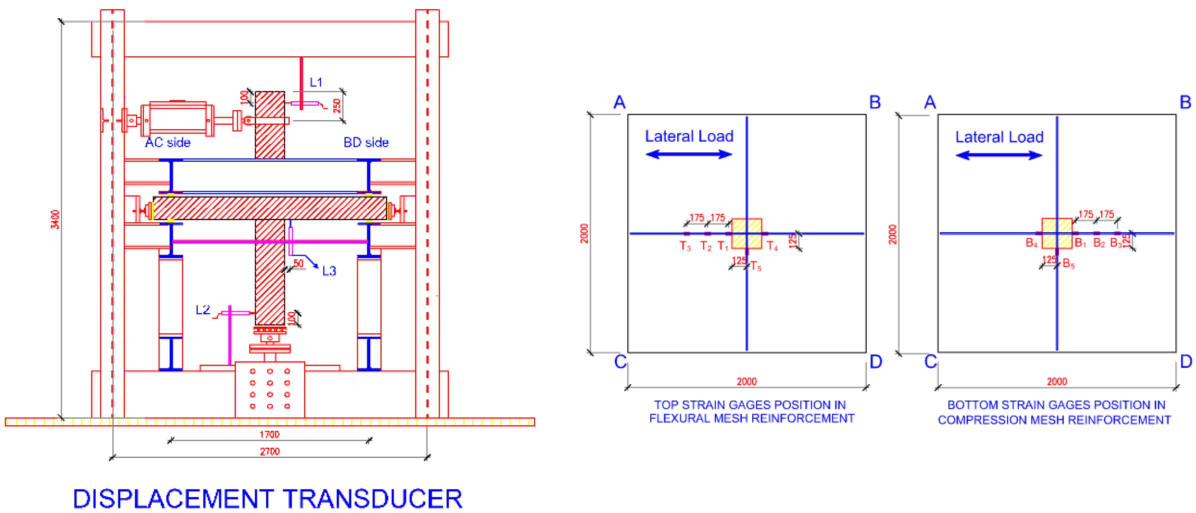

(a) LVDT to measure of Lateral drift of top and bottom column

(b) Strain gages positions in flexural mesh reinforcement

Figure 6: Instrumentation scheme for all tested specimens

V EXPERIMENTAL RESULTS

V.1-OBSERVATIONS AND CRACK PATTERN FOR SPECIMENS WITHOUT SHEAR STUDS

For specimen FP-GR-CTRL the first crack at the compression surface of the slab was observed at about a vertical gravity load equal 290 KN (about 43.5% of the failure load). For specimen FP-VR-0.4 cracks on slab surface started from corners of the column at the tension side, first on the top slab surface (which was subjected to tension from gravity load equal 230 KN) and then on the bottom surface. First crack at the bottom of the slab was observed at about 0.6~0.8% drift ratio. For specimen FP-VR-0.6 cracks on slab surface started from corners of the column at the tension side, first on the top slab surface (which was subjected to tension from gravity load equal 295 KN) and then on bottom surface. First crack at the bottom of the slab was observed at about 0.5~0.6% drift ratio. For specimen FP-VR-0.8 cracks on slab surface started from corners of the column at the tension side, first on the top slab surface (which was subjected to tension from gravity load equal 393 KN) and then on bottom surface. First crack at the bottom of the slab was observed at about 0.3~0.4% drift ratio. The final crack patterns of tension slab surfaces for tested specimens without shear studs are shown in Figure 7. All specimens failed in punching.

V.2-OBSERVATIONS AND CRACK PATTERN FOR SPECIMENS WITH SHEAR STUDS

For specimen FP-SS-0.4 (concrete compressive cylinder strength f_c*: 25MPa*) cracks on slab surface started from corners of the column at the tension side, first on the top slab surface (which was subjected to tension from gravity load equal 195 KN) and then on bottom surface. First crack at the bottom of the slab was observed at about 1.6~2.4% drift ratio. For specimen FP-SS-0.6 (concrete compressive cylinder strength f_c*: 25MPa*) cracks on slab surface started from corners of the column at the tension side, first on the top slab surface (which was subjected to tension from gravity load equal 295 KN) and then on bottom surface. First crack at the bottom of the slab was observed at about 1.1~1.6% drift ratio. Finally, for specimen FP-SS-0.8 (concrete compressive cylinder strength f_c*: 25MPa*) cracks on slab surface started from corners of the column at the tension side, first on the top slab surface (which was subjected to tension from gravity load equal 395 KN) and then on bottom surface. First crack at the bottom of the slab was observed at about 0.6~0.87% drift ratio. The final crack patterns of tension slab surfaces for tested specimens with shear studs are shown in Figure 8. All specimens failed in flexure.

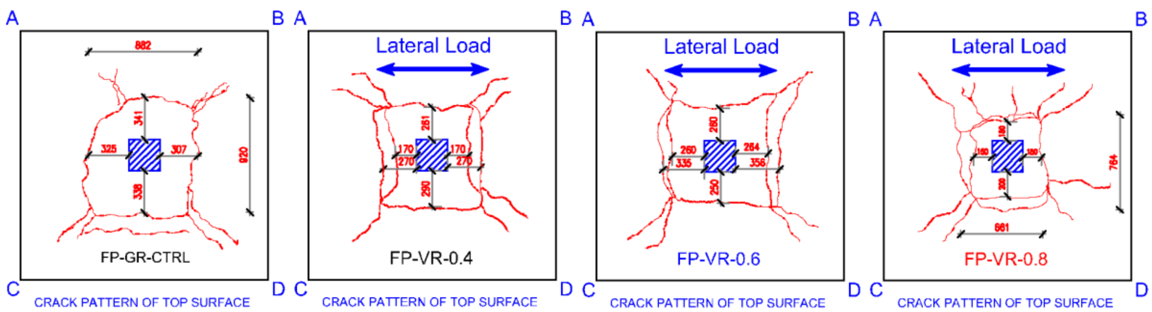

(a) FP-GR-CTRL (b) FP-VR-0.4 (c) FP-VR-0.6 (d) FP-VR-0.8

Figure 7: Crack pattern for each specimen without shear reinforcement (shear studs)

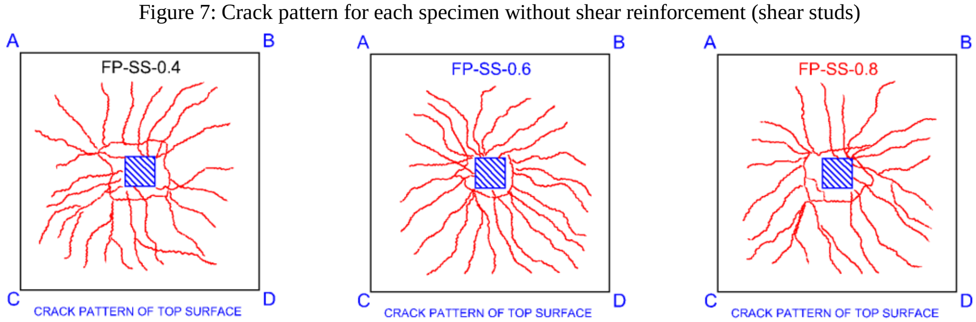

(a) FP-SS-0.4 (b) FP-SS-0.6 (c) FP-SS-0.8

Figure 8: Crack pattern for each specimen with shear reinforcement (shear studs)

V.3-LOAD-DEFLECTION CURVES

For all specimens subjected to cyclic loading, the backbone curve of the hysteresis curve of the horizontal lateral load applied at the top column end versus its horizontal lateral drift ratio is shown in Figure 9. As shown in Table 1 the peak load and drift ductility of all tested specimens, where the nominal punching shear capacity of concrete Vo= 0.333√fc bo d (ACI 318-14, in metric units). So, we conclude that the ductility capacity of specimens with studs were much higher than of specimens without shear studs, which shows that the studs contributes to improve ductility behaviour and prevents sudden brittle failure after the ultimate load. Figure 10 shows the comparisons between lateral drift ratio and lateral load, shows the gravity shear ratio level effect on lateral drift ratio and failure lateral load for all tested specimens. The backbone curve is formed by connecting peak points at the first cycle of each same-drift cycle's group. So, we conclude increasing the gravity shear ratio reduces the displacement ductility considerably as this factor is related to the connection drift capacity.

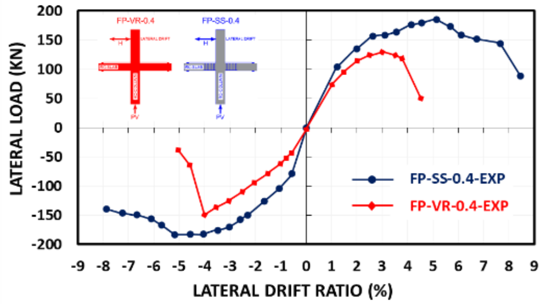

(a) FP-VR-0.4 versus FP-SS-0.4

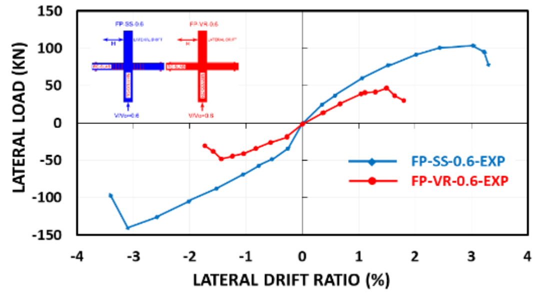

(b) FP-VR-0.6 versus FP-SS-0.6

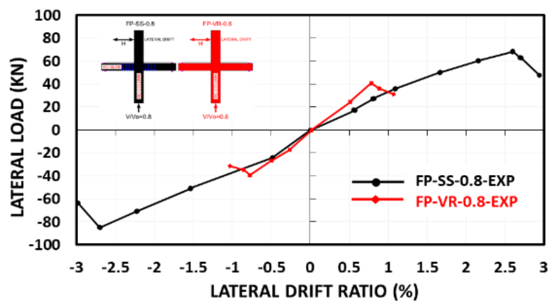

(b) FP-VR-0.8 versus FP-SS-0.8

Figure 9: backbone curve of the hysteresis curve of the horizontal load versus horizontal drift measured for all tested specimens without and with shear studs under cyclic loading

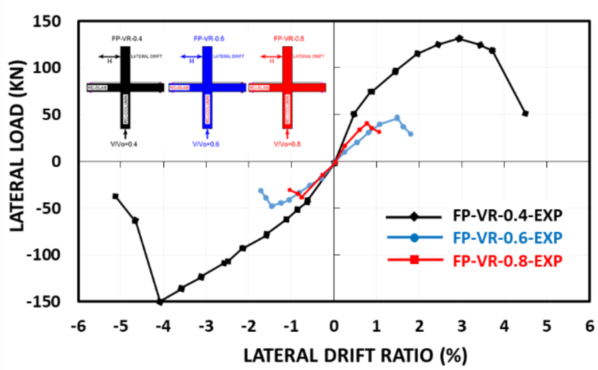

(a) All tested specimens without shear studs

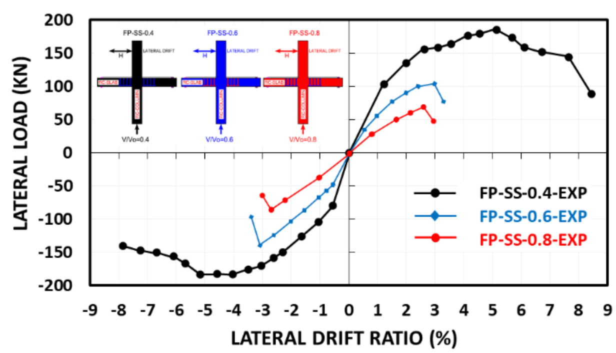

(b) All tested specimens with shear studs

Figure 10: comparisons between lateral drift ratio and lateral load,

Table 1: Peak load and drift ductility of all tested specimens under cyclic loading

SPECIMEN	V (KN)	PEAK LATERAL LOAD (KN)		HORIZONTAL DRIFT RATIO AT PEAK LATERAL LOAD (%)		YIELD DRIFT RATIO (%)		DRIFT DUCTILITY AT PEAK LATERAL LOAD μ Peak		DRIFT DUCTILITY AT 95% post PEAK LATERAL LOAD μ 0.95		DRIFTDUCTILITY AT 80% post PEAK LATERALLOAD μ 0.8	
		-	+	-	+	-	+	-	+	-	+	-	+
FP-VR-0.4	230	148	132	4	3.05	3.4	1.9	1.18	1.61	1.21	1.79	1.24	2.08
FP-VR-0.6	295	47.5	46	1.45	1.5	1.16	1.25	1.25	1.2	1.284	1.216	1.371	1.328
FP-VR-0.8	393	38	41	0.78	0.78	0.73	0.66	1.068	1.182	1.137	1.227	1.425	1.561
FP-SS-0.4	195	187	185	5.15	5.13	2.35	2.6	2.191	1.973	2.277	2.154	2.864	2.769
FP-SS-0.6	295	139	105	3.08	3	2.57	1.98	1.198	1.515	1.266	1.561	1.288	1.636
FP-SS-0.8	393	85	68.5	2.7	2.6	2.5	2.2	1.08	1.182	1.1	1.205	1.18	1.286

V.4 COMPARISON BETWEEN SHEAR STRESS AT FAILURE FROM EXPERIMENTAL RESULTS AND THEORETICAL CALCULATIONS FROM INTERNATIONAL CODES SUCH AS ACI318-14 AND EC2-2004

Figure 11 shows the critical punching shear perimeter according to ACI code and Euro code. The total shear stress ν due to direct shear V and the moment M is calculated according to Eqs. (1) ACI-318 and (2) EC2 [17]. The nominal punching shear stress resistance νc for slab – column connections without shear studs according to ACI 318-14 Eq (3) and EC2-2004.

Eq (4). The nominal punching shear stress resistance νR for slab–column connections with shear studs according to ACI 318-14 Eq (5) and EC2-2004 Eq (6).

$$\nu = \frac{V}{b_0 d} + \frac{\gamma_v M e}{J} \qquad \text{Eq (1)}$$

(a) Total shear stress due to direct shear and Moment according to ACI318-14

$$\nu = \frac{V}{u_1 d}\beta$$

$$\beta = (1 + \frac{\gamma M u_1}{V_f W_1}) \qquad \text{Eq (2)}$$

(b) Total shear stress due to direct shear and Moment according to EC2-2004

where γ_v is the fraction of M transferred by shear, e is the distance from the centroid of the critical section to the point where shear stress is calculated, J is the analogous polar moment of inertia of the shear critical section, β is the increase in shear stresses due to the unbalanced moment for one direction moment, bo and u1 are the perimeters of the critical shear section, γ is a coefficient based on the ratio between the column dimension for a square column γ = 0.6) and W1 corresponds to a distribution of shear and is a function of the basic perimeter. For a rectangular column W1 is given as:

$$W_1 = \frac{c_1^2}{2} + c_1 c_2 + 4c_2 d + 16d^2 + 2\pi d c_1$$

Where, C1 is the column dimension parallel to the eccentricity of the load and C2 is the dimension of the column that is perpendicular to the eccentricity of the load.

$$\nu_C = 0.333\sqrt{fc} \qquad \text{Eq (3)}$$

(c) Nominal punching shear capacity without Shear studs according to ACI318-14

$$\nu_C = 0.18k(100\rho f_{ck})^{\frac{1}{3}} \qquad \text{Eq (4)}$$

(d) Nominal punching shear capacity without Shear studs according to EC2-2004

$$\nu_R = 0.5Vc + \frac{Astuds * fys}{bo * s} \leq 0.66\sqrt{fc} \qquad \text{Eq (5)}$$

(e) Nominal punching shear capacity with Shear studs according to ACI318-14

$$\nu_R = 0.75Vc + 1.5\frac{Astuds * fywd,ef}{bo * s}$$

$$K = 1 + (200/d)^{\frac{1}{2}}$$

$$fywd, ef = (250 + 0.25d) \leq fys \qquad \text{Eq (6)}$$

(f) Nominal punching shear capacity with Shear studs according to EC2-2004

Where, Astuds is the area of one row of the vertical shear reinforcement, s is the spacing between the perimeters of shear studs, $f$ys is the yield strength of the shear studs. and $fywd$, is the effective design strength of the shear studs

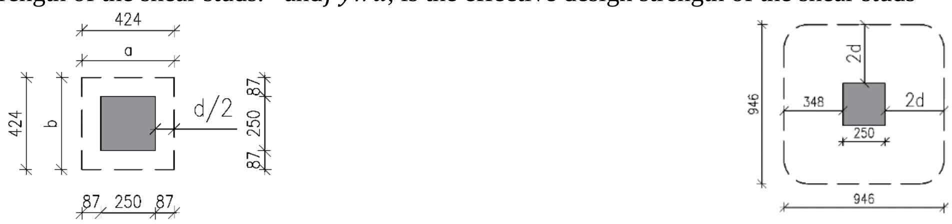

(a) According to ACI318-14 (b) According to EC2-2004

Figure 11: Punching shear perimeter according to ACI code and Euro code

Table 2 compares the experimental results with the code provisions. It can be concluded that for the specimen without applied moment the codes accurately predict the shear resistance. However, for the specimens with moment transfer the codes (especially EC2) overestimates the resistance of the tested specimens.

Table 2: Failure shear stress (N/mm^2) according to **ACI318-14** and **EC2-2004**

Specimen	f'_c **(N/mm^2)**	**ACI318-14**			**EC2-2004**		
		v_r **(N/mm^2)**	v_{test} **(N/mm^2)**	**Ratio** v_{test}/v_r	v_r **(N/mm^2)**	v_{test} **(N/mm^2)**	**Ratio** v_{test}/v_r
FP-GR-CTRL	**27**	**1.732**	**2.26**	**1.305**	**1.268**	**1.203**	**0.949**
FP-VR-0.4	**35**	**1.972**	**1.801**	**0.913**	**1.383**	**0.788**	**0.570**
FP-VR-0.6	**25**	**1.667**	**1.317**	**0.790**	**1.236**	**0.648**	**0.524**
FP-VR-0.8	**25**	**1.667**	**1.608**	**0.965**	**1.236**	**0.809**	**0.655**
FP-SS-0.4	**25**	**3.334**	**1.952**	**0.585**	**2.397**	**0.823**	**0.344**
FP-SS-0.6	**25**	**3.334**	**2.035**	**0.610**	**2.397**	**0.911**	**0.380**
FP-SS-0.8	**25**	**3.334**	**1.918**	**0.575**	**2.397**	**0.923**	**0.385**

Equation (Eq.7) of ACI318-14 determines the zone in which shear reinforcement is required as a relation between the ultimate design drift ratio DRu and the gravity shear ratio V/V0.

$$DRu = 0.035 - 0.05*(V/Vo) \text{ for } (V/Vo \leq 0.6), \qquad DRu = 0.005 \text{ for } (V/Vo \geq 0.6) \qquad \text{Eq (7)}$$

Fig. 12 includes drift results of all tested specimens as a function of V/Vo as well as Eq. 7. The gravity shear resistance Vo was calculated in three different ways: according to ACI 314, EC 2 and from the control test FP-GR-CTRL. The results indicate that the drift ratio was achieved without shear reinforcement in contrary to the ACI requirements. Equation 7 of ACI 318 seems to be in a better match with the shear stresses calculated according to EC 2.

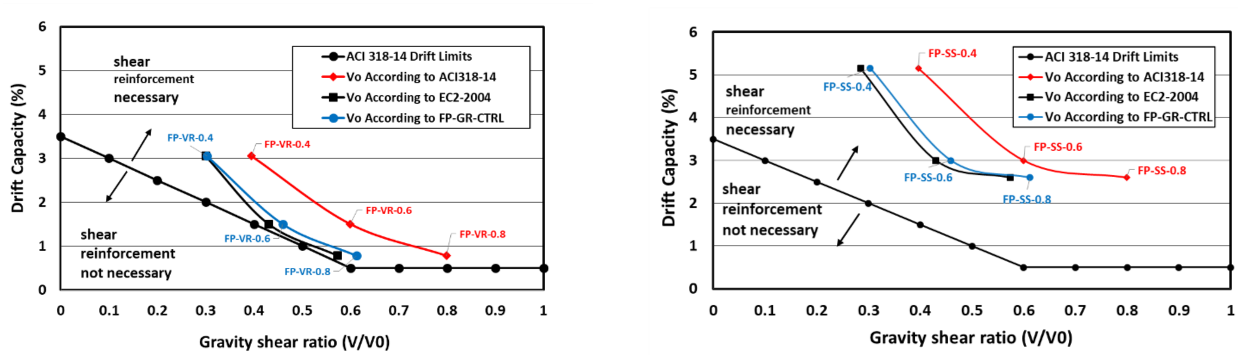

(a) All specimens without shear studs (b) All specimens with shear studs

Figure 12: Maximum drift ratio DRu achieved for interior slab-column connections tested without and with shear reinforcement (shear studs)

VI. Conclusion

This paper presents the results of an experimental investigation of the effect shear studs on the punching shear response of interior slab-column connections under seismic loading. The following are the main conclusions.

1- Increasing the gravity shear ratio reduces the displacement ductility considerably as this factor is related to the connection drift capacity.

2- The experimental results showed that the punching shear resistance of the slab-column connections are reduced if subjected to lateral cyclic loading in addition to the vertical load.

3- The code provisions of ACI318-14 and EC2-2004 predicted accurately the failure loads for reference control specimen subjected to gravity shear only, while overestimated the failure loads for all other specimens under reversed cyclic moments.

4- Tests subjected to cyclic moments indicate that the anticipated drift ratio can be achieved without shear reinforcement indicating conservative provisions of ACI 318-14 in this regard.

5- The tests results confirmed the trend of the ACI equation relating the drift capacity with the level of gravity shear for connections subjected to cyclic moments in addition to gravity shear. The ACI equation shows better agreement with the test results if the shear stresses are calculated according to EC 2.

6- Shear studs can change failure mode of the flat slab column connections. Slabs properly with shear studs will exhibit desirable flexural while slabs without shear studs can be subjected to abrupt punching shear failure.

7- The specimens with shear studs can undergo more lateral drift cycles at large deformation, showing a significant increase in energy dissipation capacity.

8- The ductility capacity of specimens with studs were much higher than of specimens without shear studs, which shows that the studs contribute to improve ductility behaviour and prevents sudden brittle failure after the ultimate load.

REFERENCES

[1] Megally, S., and Ghali, A., “Punching Shear Design of Earthquake-Resistant Slab-Column Connections”, ACI Structural Journal, 97, 5, Sept.-Oct. 2002, pp. 720-730.

[2] Megally, S., and Ghali, A., “Punching Shear Design of Earthquake-Resistant Slab-Column Connections”, ACI Structural Journal, 97, 5, Sept.-Oct. 2002, pp. 720-730.

[3] Cheng M. Y., “Punching shear strength and deformation capacity of fiber reinforced concrete slabcolumn connections under earthquake loading,” PhD Dissertation, Al-Rasheed Civil Engineering Department, the University of Michigan, United States, 2009.

[4] Changsoon, R., Kang, T. H. K., Shin, M., and Yoon, J. B., “Gravity and lateral load-carrying capacities of reinforced concrete flat plate systems,” ACI Structural Journal, vol. 111, no. 4, pp. 753–764, 2014.

[5] Matzke, E. M., Lequesne, R. D.m Parra-Montesinos, G. J. and Shield, C. K., “Behavior of biaxially loaded slab-column connections with shear stud,” ACI Structural Journal, vol. 112, no. 3, pp. 335–346, 2015.

[6] Erberik, M. A., and Elnashai, A. S., “Fragility analysis of flat-slab structures,” Engineering Structures, vol. 26, pp. 937–948, 2004.

[7] Robertson, I., and Durrani, A. J., “Gravity load effect on seismic behavior of exterior slab-column connections,” ACI Structural Journal, vol. 88, no. 3, pp. 255–267, 1991

[8] Robertson, I., and Durrani, A. J., “Gravity load effect on seismic behavior of interior slab-column connections,” ACI Structural Journal, vol. 89, no. 1, 37–45, 1993.

[9] Robertson, I., Kawai, T., Lee, J., Enomoto, B., “Cyclic testing of slab-column connections with shear reinforcement,” ACI Structural Journal, vol. 99, no. 5, pp. 605–613, 2002.

[10] Robertson, I., and Johnson, G., “Cyclic lateral loading of nonductile slab-column connections,” ACI Structural Journal, vol. 103, no. 3, pp. 356–364, 2006.

[11] Gunadi, R., Budiono, B., Imran, I., and Sofwan, A., “Peningkatan perilaku hubungan pelat-kolom terhadap beban lateral siklis dengan menggunakan detail tulangan geser baru,” Prosiding Konferensi Nasional Pascasarjana Teknik Sipil (KNPTS), pp. 66–76, 2012.

[12] Dilger, W. H. and Ghali, A. (1981). Shear reinforcement for concrete slabs. Journal of Structural Division 107:12, 2403-2420.

[13] Megally, S. and Ghali, A. (2000). Seismic behavior of slab-column connections. Canadian Journal of Civil Engineering. 27:1, 84-100.

[14]

[15] Pan, A. A. and Moehle, J. P. (1988). Reinforced Concrete Flat Plates under Lateral Loadings: An Experimental Study Including Biaxial Effects. Report. No. UCB/EERC-88/16, Earthquake Engineering Research Center, Univ. of California at Berkeley, Berkeley, Calif.

[16] Widianto, Bayrak, O., and Jirsa, J. O. (2009). Two-way shear strength of slab-column connections: Reexamination of ACI 318 provisions. ACI Structural Journal 106:2, 160-170.

[17] ACI 318-14, “Building Code Requirements for Structural Concrete and Commentary”, American Concrete Institute, Farmington hills, 2014.

[18] European Standard, “Eurocode 2: Design of concrete structures”, CEN, European Standard, 2004

[19]